

# Topology optimization of a novel fuselage structure in the conceptual design phase

## Abstract

### *Purpose*

– In recent years, innovative aircraft designs have been investigated by researchers to address the environmental and economic issues for the purpose of green aviation. To keep air transport competitive and safe, it is necessary to maximize design efficiencies of the aircrafts in terms of weight and cost. The purpose of this paper focuses on the research which has led to the development of a novel lattice-fuselage design of a forward-swept wing aircraft in the conceptual phase by topology optimization technique.

### *Design/methodology/approach*

– In this paper, the fuselage structure is modelled with two different types of elements -1D beam and 2D shell- for the validation purpose. Then, the finite element analysis coupled with topology optimization is performed to determine the structural layouts indicating the efficient distributed reinforcements. Following that, the optimal fuselage designs are obtained by comparison of the results of 1D and 2D models.

### *Findings*

– The topological results reveal the need for horizontal stiffeners to be concentrated near the upper and lower extremities of the fuselage cross section and a lattice pattern of criss-cross stiffeners should be well-placed along the sides of the fuselage and near the regions of window locations. The slight influence of windows on the optimal reinforcement layout is observed. To form clear criss-cross stiffeners, modelling the fuselage with 1D beam elements is suggested, whereas the less computational time is required for the optimization of the fuselage modelled using 2D shell elements.

### *Originality/value*

– The authors propose a novel lattice fuselage design in use of topology optimization technique as a powerful design tool. Two types of structural elements are examined in order to obtain the clear reinforcement detailing, which is also in agreement with the design of the DLR (German Aerospace Center) demonstrator. The optimal lattice layout of the stiffeners is distinctive to the conventional semi-monocoque fuselage design and this definitely provides valuable insights into the more efficient utilization of composite materials for novel aircraft designs.

**Keywords:** Lattice pattern, Composite fuselage, Topology optimization; Conceptual design

## Introduction

Composite lattice filament-wound tubular structures have been successfully applied for many years by Russian rocket designers due to their excellent strength and stiffness to weight ratios (Vasiliev *et al.* 2001, 2006). Innovative aircraft designs, like Airbus A350, the integrated airplane layout with new performance synergies (Seitz *et al.* 2014), and Blended Wing Bodies (Russell *et al.* 2010), have been investigated to address the environmental and economic considerations for the purpose of green aviation. As metal designs of primary load-bearing structures, for example aircraft fuselages, have reached their climax after 90 years of development in the field of aerospace engineering, it is really challenging to achieve extraordinary weight and cost savings based on the conventional design of commercial aircraft fuselages produced by semi-monocoque construction (Shanygin *et al.* 2012). To tackle this problem, the potentials of extremely lightweight, high-strength fiber reinforced composites and innovative reinforcement configurations should be further explored in the design of aircraft fuselages. Carbon fibre reinforced plastics have very successful applications in aerospace industries in recent years and they outperform aluminium alloys in terms of very high strength and rigidity (Quilter 2004, Daniel and Ishai 2005). However, the potential of composites has not been completely exploited due to the simple use of conventional aircraft airframe layouts as design principles (Ostrower 2011).

The composite lattice structure was developed and produced by the Russian Central Research Institute for Special Machinery (CRISM) for rocket structures (Wilmes *et al.* 2002, Herbeck *et al.* 2003, Kolesnikov and Herbeck 2004, Vasiliev *et al.* 2012) in the 1980s. These structures consist of ribs either helically or ring-shaped, which are made of unidirectional composite fibres using automatic filament winding. Such structures are known as lattice or anisogrid structures shown in Figure 1. The advanced mechanical properties of the unidirectional composites of the lattice ribs are the main factor to strive for their high weight efficiency, while the skin of the cylindrical or conical shells is usually manufactured to carry an insignificant part of the loading, such as tension, compression and shear. As the automatic filament winding process technique has been well developed to produce composites, an integral structure with a low manufacturing cost is ensured. These achievements open up new opportunities for the optimal design of composite aircraft fuselage barrels (Shanygin *et al.* 2012, Vasiliev *et al.* 2012).



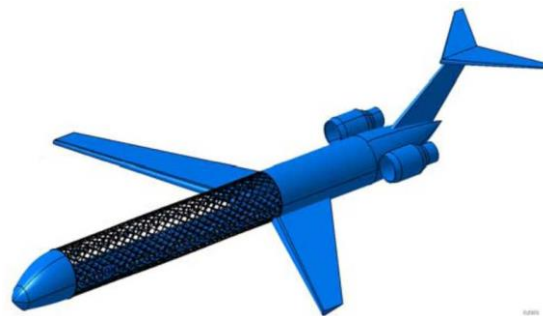
Figure 1 A barrel in a lattice structure developed for the rocket engineering application

Taking these situations into account, a full-scale load-bearing lattice structure (Wilmes *et al.* 2002, Herbeck *et al.* 2003, Vasiliev *et al.* 2012) was developed as a demonstrator by CRISM and DLR

1  
2  
3 (German Aerospace Center) in the field of Rocket Engineering. However, the implementation of  
4 composite lattice structures into the commercial aircraft is still an issue. To address this challenging  
5 problem, a comprehensive investigation starting with the beneficial geodesic design well-proven in  
6 space technology and transferring it to commercial composite aircraft fuselage designs was  
7 performed in the project entitled Advanced Lattice Structures for Composite Airframes (ALasCA  
8 2013).

9  
10  
11 Topology optimization technique (Bendsøe and Sigmund 2003) has been widely used in various  
12 engineering disciplines (Zhou 2002, Harzheim and Graf 2005), especially aeronautical and  
13 aerospace engineering (Krog *et al.* 2002 and 2004, James *et al.* 2014, Rao *et al.* 2008, Zhou *et al.*  
14 2010, Zhu *et al.* 2016). Topology optimization is a finite element based structural optimization  
15 process, increasingly used by engineers to support the development of minimum weight structures.  
16 With respect to the design objectives, the aim of topology optimization is to identify the most  
17 advantageous material distribution inside the design domain. Its methods, theory and various  
18 applications have been recently discussed by Deaton and Grandhi (2014).  
19  
20  
21

22 In this paper, the aircraft configuration and loads applied in the DLR funded project LamAiR (Seitz  
23 *et al.* 2011) are used to model the fuselage of a forward-swept wing aircraft shown in Figure 2 with  
24 two different types of elements: 1D beam and 2D shell. Following that, the integration of structural  
25 analysis with topology optimization is applied to determine the efficient material layouts indicating  
26 the structural reinforcements for the fuselage with and without windows, respectively. Subsequently,  
27 the influences of element types and windows on the optimal fuselage design in the conceptual phase  
28 are studied. Finally, a lightweight and cost effective lattice fuselage design is practically developed  
29 based considering the topological results and manufacturability of the reinforcements.  
30  
31  
32



33  
34  
35  
36  
37  
38  
39  
40  
41  
42  
43  
44  
45  
46  
47  
48 Figure 2 Forward-swept wing aircraft concepts with a long undisturbed lattice fuselage

### 49 50 51 **Topology optimization technique**

52 Topology optimization is the most general type of structural optimization, being performed in the  
53 initial phases of the design. It is a mathematical approach that optimizes the material layout or  
54 distribution subject to some constraints in a given design space to achieve the minimum weight  
55

structures or the most efficient designs. Topology optimization methods for continuum structures seek an optimal material distribution, which defines both the external boundaries of the structure and the number, position, size and shape of internal holes in the structure. In the conventional aircraft fuselage design, the fuselage stiffeners are commonly arranged in the same direction as the axis of the fuselage and are also evenly distributed along its circumference. Such a fuselage is reinforced by longitudinal stringers and constructed by semi-monocoque technique (Airframe 2012), while the utilization of composite materials potentially allows for these stiffeners to be arranged along any axis (Vasiliev *et al.* 2006, 2012) as well as achieved in a significant reduction in weight. This is the logic behind why topology optimization technique is proposed in this paper to seek the innovative fuselage design of a forward-swept wing aircraft. In order to provide a scientific basis for finding a rational structural layout for the fuselage design, the Solid Isotropic Material with Penalisation (SIMP) (Bendsøe 1989, Bendsøe and Sigmund 2003, Mlejnek 1992, Sigmund 2001, Zhou and Rozvany 1991) topology optimization method is used to determine the efficient stiffener arrangements.

In a very simple formulation of the topology optimization problem, the artificial material is defined to have a variable material density  $\rho$  and an associated variable stiffness  $E(\rho, \rho) = \rho^q E$  for each finite element in a design space of the model. Taking  $E$  as the stiffness of an isotropic material, a design description that allows each finite element represented by either a void “ $\rho = 0$ ” or material “ $\rho = 1$ ” is achieved. Using this simple formulation, topology optimization for the design with a minimum total elastic energy  $U_e$  as the objective function can be simply written as:

$$\begin{aligned} \min \quad & U_e \\ \text{subject to} \quad & \sum_{n=1}^N \rho_n V_n \leq V_0 \\ & n = 1, \dots, N \\ & \rho_{\min} \leq \rho \leq 1 \end{aligned} \quad (1)$$

where  $U_e$  is the total elastic energy for the structure;  $N$  is the total number of finite elements in the designable area;  $n$  is the number of the analysed finite element;  $\rho$  is the design variable and artificial element density used by the SIMP method to tailor structural stiffness of each finite element in the structure.

The above provides a classical total elastic energy based topology optimization formulation, which can be also considered as a maximum stiffness or minimum compliance design problem. Normally the buckling requirement is not considered in this stage, but the ‘topologically optimized’ design should be further fine-tuned afterwards by shape and size optimization methods regarding the stability constraint.

### Forward-swept wing aircraft configuration and loads

In this section, the aircraft configuration from the project LamAir (Seitz *et al.* 2011) was used to model the fuselage, cargo and passenger floors, and struts of a forward-swept wing aircraft for structural analysis and topology optimization in use of Altair OptiStruct (2013). The passenger and cargo doors are naturally large cut-outs, which is one of the main features of the forward-swept wing aircraft. These doors are placed in the front cockpit-section and behind the wing, respectively.

Considering this character, a long undisturbed barrel section can be reasonably defined as the designable part in the optimization process and this would lead to a lightweight and cost-efficient fuselage design.

The length of the fuselage section was 13,652 mm and it included two introduction bays, each of which was 399.8 mm in length. The rest of the fuselage had 22 bays and the pitch length between two adjacent bays was 584.2 mm shown in Figure 3. The cross section was made from three different radii and included a passenger and a cargo floors with struts connecting the floors, see Figure 4.

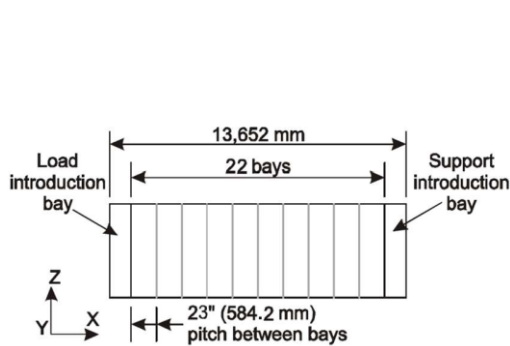


Figure 3 The fuselage configuration

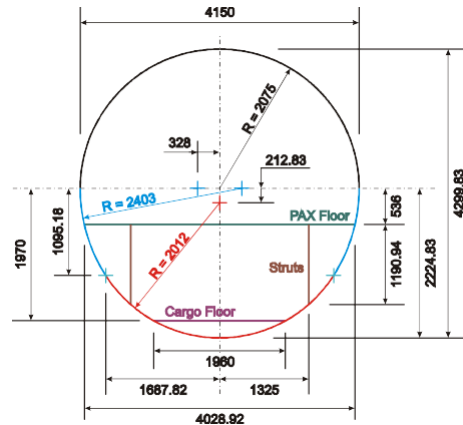


Figure 4 Geometrical parameters of fuselage cross-section

An upward gust load was applied to the fuselage of the forward-swept wing aircraft flying at low altitude, cruise speed. There were three sources of loads: 1) gravitational forces resulting from the uniformly distributed masses on the fuselage and its ring frames, 2) point loads and moments at the free end of the fuselage cross section, and 3) uniformly distributed point loads on the passenger and cargo floors along the fuselage axis. The second group of loads applied at the free end was shown in Figure 5 and it included seven concentrated loads, four of which were gravitational forces representing the passenger floor mass and three resulting from the cargo floor mass. The third group of loads was depicted in Figure 6. Based on these loads, three load cases and magnitudes of loads were defined in Table 1 and they were applied on the fuselage to perform the structural analysis and topology optimization. In Load Case 1 (LC 1), there was a load factor of 3.47 acting in the negative z-direction on the mass of the fuselage, ring frames, passenger floor, and cargo floor. A vertical shear force  $Q_z$  and moment  $M_y$  were also considered. This retained Load Case 1 a critical load case in the design process. Load Case 2 included a horizontal shear force  $Q_y$  and a bending moment  $M_z$ . Load Case 3 consisted of a torque  $T$  about the x-axis applied in either directions.

In the finite element modelling of fuselage section, the fuselage mass was evenly distributed over the entire fuselage elements and this was achieved by assigning the element with the non-

structural mass property. The ring frames mass in Figure 3 was evenly distributed over the 23 rings. The passenger and cargo floor masses were applied on the fuselage section with the magnitudes  $F_{PAX}$ ,  $F_{Cargo Latches}$  and  $F_{Cargo Central}$  given by Eqs 2, 3, and 4

$$F_{PAX} = \frac{g_{LC} \times M_{PAX Total}}{4 \times N_{Frames}} \quad (2)$$

$$F_{Cargo Central} = \frac{g_{LC} \times M_{Cargo Total}}{2 \times N_{Frames}} \quad (3)$$

$$F_{Cargo Latches} = \frac{g_{LC} \times M_{Cargo Total}}{4 \times N_{Frames}} \quad (4)$$

where:

$F_{PAX_i}$  means point force on passenger floor for  $i^{th}$  load case

$g_{LC}$  is the acceleration for  $i^{th}$  load case

$M_{PAX Total_i}$  represents the total mass acting on the passenger floor for  $i^{th}$  load case

$N_{Frames}$  is the number of ring frames in the model and 23 (this means 22 number of bays in total) are used in this paper. However, this could vary from the number required for a 508 mm to a 787.4 mm pitch length.

$F_{Cargo Central_i}$  represents the central point force on the cargo floor for  $i^{th}$  load case

$M_{Cargo Total}$  represents the total mass acting on the cargo floor for  $i^{th}$  load case

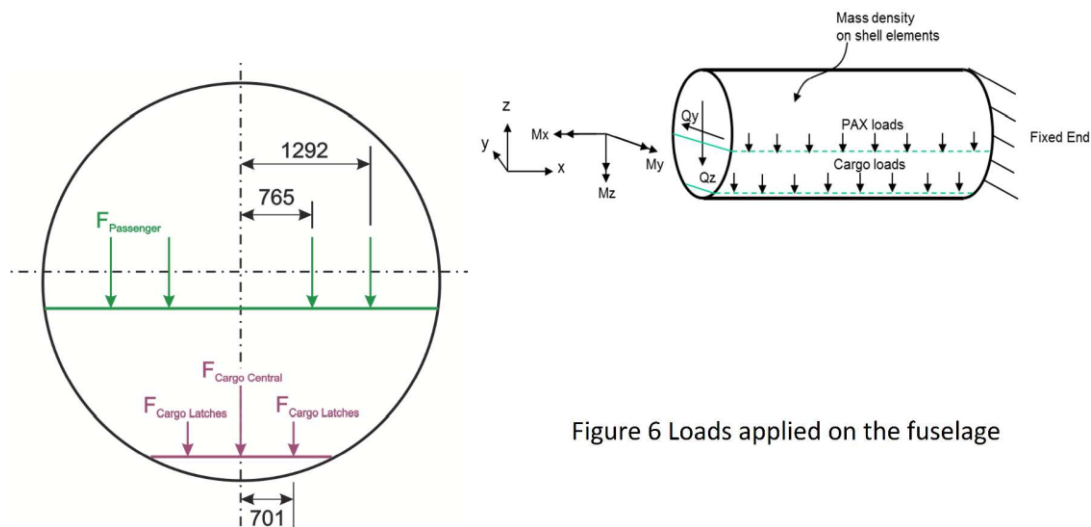


Figure 6 Loads applied on the fuselage

Figure 5 Loads on the passenger and cargo floors in the plane of fuselage cross-section

Table 1 Three load cases applied on the fuselage section

Load Case	$Q_z$ (N)	$M_y$ (Nm)	T ( $M_x$ , Nm)	$Q_y$ (N)	$M_z$ (Nm)
1 (downwards loads)	211,711	446,965	-	-	-
2 (sideways loads)	-	-	-	$\pm 80,000$	+ 249,614
3 (torsional load)	-	-	$\pm 280,000$	-	-

**Finite Element (FE) modeling and boundary conditions**

The study of fundamental properties of the optimal grid-like pattern in Figure 7 was made by many researchers (Michell 1904, Prager 1974, Rozvany *et al.* 1993 and 1995, Rozvany 1998). Motivated by Michell’s work, intuitive methods of analysing and designing the fuselage structure modelled with 1D beam and 2D shell elements for a maximum stiffness under a given weight are employed in this paper. Since the results obtained by topology optimization can’t be applied directly in the practical design process, structural interpretation of topological results using mechanics concepts is given to identify a clear, efficient reinforcement layout for the fuselage of the preceding forward-swept wing aircraft. Also, the influence of windows on the optimal design under the mentioned three load cases in Section *Forward-swept wing aircraft configuration and loads* are discussed in Section *Lattice fuselage design of a forward-swept wing aircraft*.

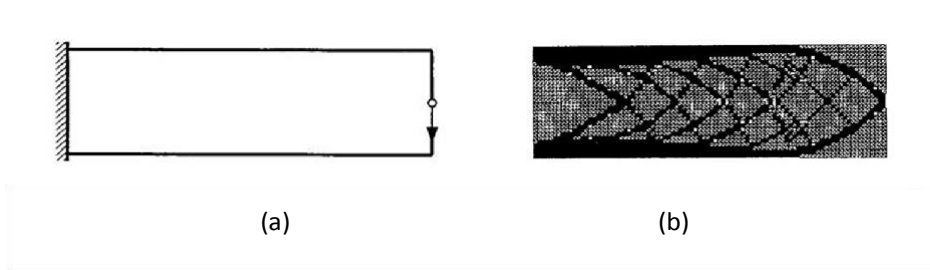


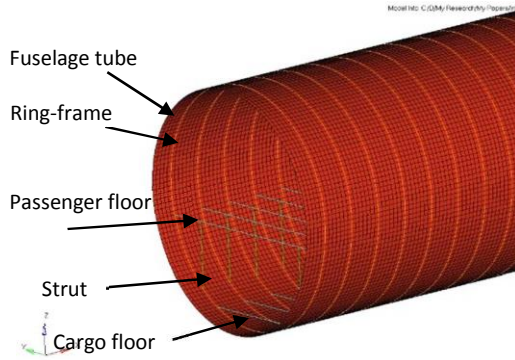
Figure 7 (a) The Michell cantilever; (b) The generalized shape of a perforated

**Fuselage section without cut-outs**

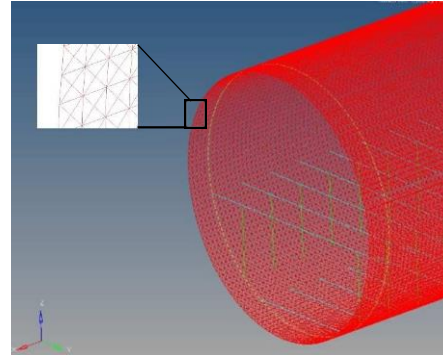
In the detailed FE model of the fuselage without windows shown in Figures 8 and 9, **25584 2D shell**



1  
2  
3 **elements (4-node)** and 179088 1D beam element (2-node) were used to construct the fuselage  
4 structure, respectively. The passenger floor, cargo floor and struts were modelled with 2254 rod  
5 elements (2-node), which only carried the axial forces. The ring frames of the fuselage were  
6 modelled with 3588 beam elements (2-node), which bore not only axial forces but out-of-plane  
7 forces. The logic behind the structural components being modelled as above was to identify the  
8 efficient pattern on the skin of the fuselage tube by assigning loads to the primary load-bearing  
9 structures - the reinforcement ribs. At two ends of the fuselage section, there are two introduction  
10 bays to reduce the local effects (loading and boundary conditions) on the final results.



11  
12  
13  
14  
15  
16  
17  
18  
19  
20  
21  
22  
23  
24  
25  
26  
27  
28  
29 Figure 8 FE modelling of the fuselage tube without  
30 windows using shell elements



31  
32  
33  
34  
35  
36  
37  
38  
39  
40  
41  
42  
43  
44  
45  
46  
47  
48  
49  
50  
51  
52  
53  
54  
55 Figure 9 FE modelling of the fuselage  
56 tube without windows using beam  
57 elements

### 58 **Fuselage section with cut-outs**

59  
60  
61  
62  
63  
64  
65  
66  
67  
68  
69  
70  
71  
72  
73  
74  
75  
76  
77  
78  
79  
80  
81  
82  
83  
84  
85  
86  
87  
88  
89  
90  
91  
92  
93  
94  
95  
96  
97  
98  
99  
100  
101  
102  
103  
104  
105  
106  
107  
108  
109  
110  
111  
112  
113  
114  
115  
116  
117  
118  
119  
120  
121  
122  
123  
124  
125  
126  
127  
128  
129  
130  
131  
132  
133  
134  
135  
136  
137  
138  
139  
140  
141  
142  
143  
144  
145  
146  
147  
148  
149  
150  
151  
152  
153  
154  
155  
156  
157  
158  
159  
160  
161  
162  
163  
164  
165  
166  
167  
168  
169  
170  
171  
172  
173  
174  
175  
176  
177  
178  
179  
180  
181  
182  
183  
184  
185  
186  
187  
188  
189  
190  
191  
192  
193  
194  
195  
196  
197  
198  
199  
200  
201  
202  
203  
204  
205  
206  
207  
208  
209  
210  
211  
212  
213  
214  
215  
216  
217  
218  
219  
220  
221  
222  
223  
224  
225  
226  
227  
228  
229  
230  
231  
232  
233  
234  
235  
236  
237  
238  
239  
240  
241  
242  
243  
244  
245  
246  
247  
248  
249  
250  
251  
252  
253  
254  
255  
256  
257  
258  
259  
260  
261  
262  
263  
264  
265  
266  
267  
268  
269  
270  
271  
272  
273  
274  
275  
276  
277  
278  
279  
280  
281  
282  
283  
284  
285  
286  
287  
288  
289  
290  
291  
292  
293  
294  
295  
296  
297  
298  
299  
300  
301  
302  
303  
304  
305  
306  
307  
308  
309  
310  
311  
312  
313  
314  
315  
316  
317  
318  
319  
320  
321  
322  
323  
324  
325  
326  
327  
328  
329  
330  
331  
332  
333  
334  
335  
336  
337  
338  
339  
340  
341  
342  
343  
344  
345  
346  
347  
348  
349  
350  
351  
352  
353  
354  
355  
356  
357  
358  
359  
360  
361  
362  
363  
364  
365  
366  
367  
368  
369  
370  
371  
372  
373  
374  
375  
376  
377  
378  
379  
380  
381  
382  
383  
384  
385  
386  
387  
388  
389  
390  
391  
392  
393  
394  
395  
396  
397  
398  
399  
400  
401  
402  
403  
404  
405  
406  
407  
408  
409  
410  
411  
412  
413  
414  
415  
416  
417  
418  
419  
420  
421  
422  
423  
424  
425  
426  
427  
428  
429  
430  
431  
432  
433  
434  
435  
436  
437  
438  
439  
440  
441  
442  
443  
444  
445  
446  
447  
448  
449  
450  
451  
452  
453  
454  
455  
456  
457  
458  
459  
460  
461  
462  
463  
464  
465  
466  
467  
468  
469  
470  
471  
472  
473  
474  
475  
476  
477  
478  
479  
480  
481  
482  
483  
484  
485  
486  
487  
488  
489  
490  
491  
492  
493  
494  
495  
496  
497  
498  
499  
500  
501  
502  
503  
504  
505  
506  
507  
508  
509  
510  
511  
512  
513  
514  
515  
516  
517  
518  
519  
520  
521  
522  
523  
524  
525  
526  
527  
528  
529  
530  
531  
532  
533  
534  
535  
536  
537  
538  
539  
540  
541  
542  
543  
544  
545  
546  
547  
548  
549  
550  
551  
552  
553  
554  
555  
556  
557  
558  
559  
560  
561  
562  
563  
564  
565  
566  
567  
568  
569  
570  
571  
572  
573  
574  
575  
576  
577  
578  
579  
580  
581  
582  
583  
584  
585  
586  
587  
588  
589  
590  
591  
592  
593  
594  
595  
596  
597  
598  
599  
600  
601  
602  
603  
604  
605  
606  
607  
608  
609  
610  
611  
612  
613  
614  
615  
616  
617  
618  
619  
620  
621  
622  
623  
624  
625  
626  
627  
628  
629  
630  
631  
632  
633  
634  
635  
636  
637  
638  
639  
640  
641  
642  
643  
644  
645  
646  
647  
648  
649  
650  
651  
652  
653  
654  
655  
656  
657  
658  
659  
660  
661  
662  
663  
664  
665  
666  
667  
668  
669  
670  
671  
672  
673  
674  
675  
676  
677  
678  
679  
680  
681  
682  
683  
684  
685  
686  
687  
688  
689  
690  
691  
692  
693  
694  
695  
696  
697  
698  
699  
700  
701  
702  
703  
704  
705  
706  
707  
708  
709  
710  
711  
712  
713  
714  
715  
716  
717  
718  
719  
720  
721  
722  
723  
724  
725  
726  
727  
728  
729  
730  
731  
732  
733  
734  
735  
736  
737  
738  
739  
740  
741  
742  
743  
744  
745  
746  
747  
748  
749  
750  
751  
752  
753  
754  
755  
756  
757  
758  
759  
760  
761  
762  
763  
764  
765  
766  
767  
768  
769  
770  
771  
772  
773  
774  
775  
776  
777  
778  
779  
780  
781  
782  
783  
784  
785  
786  
787  
788  
789  
790  
791  
792  
793  
794  
795  
796  
797  
798  
799  
800  
801  
802  
803  
804  
805  
806  
807  
808  
809  
810  
811  
812  
813  
814  
815  
816  
817  
818  
819  
820  
821  
822  
823  
824  
825  
826  
827  
828  
829  
830  
831  
832  
833  
834  
835  
836  
837  
838  
839  
840  
841  
842  
843  
844  
845  
846  
847  
848  
849  
850  
851  
852  
853  
854  
855  
856  
857  
858  
859  
860  
861  
862  
863  
864  
865  
866  
867  
868  
869  
870  
871  
872  
873  
874  
875  
876  
877  
878  
879  
880  
881  
882  
883  
884  
885  
886  
887  
888  
889  
890  
891  
892  
893  
894  
895  
896  
897  
898  
899  
900  
901  
902  
903  
904  
905  
906  
907  
908  
909  
910  
911  
912  
913  
914  
915  
916  
917  
918  
919  
920  
921  
922  
923  
924  
925  
926  
927  
928  
929  
930  
931  
932  
933  
934  
935  
936  
937  
938  
939  
940  
941  
942  
943  
944  
945  
946  
947  
948  
949  
950  
951  
952  
953  
954  
955  
956  
957  
958  
959  
960  
961  
962  
963  
964  
965  
966  
967  
968  
969  
970  
971  
972  
973  
974  
975  
976  
977  
978  
979  
980  
981  
982  
983  
984  
985  
986  
987  
988  
989  
990  
991  
992  
993  
994  
995  
996  
997  
998  
999  
1000

The barrel with cut-outs representing the windows in Figure 10 was modelled with 25100 2D shell elements and 150580 1D beam element, respectively. The pitch length (the distance between two adjacent ring frames) could vary from 508 mm (minimum distance) to 787.4 mm (maximum distance). In this study, the frame pitch length of 584.2mm was evaluated and the detailed information about window geometry was described in Figure 11.



Figure 10 The fuselage with windows



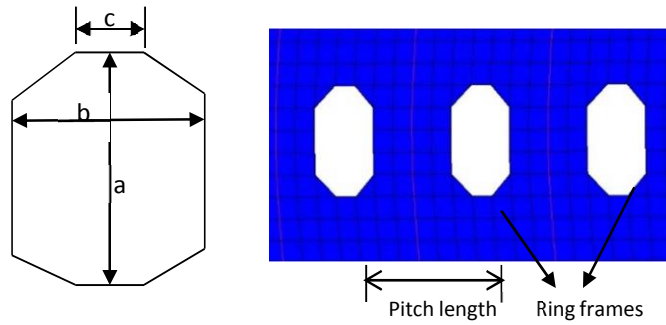


Figure 11 Pitch length and window position in the fuselage section and geometry of cut-outs:  $a=420.35\text{mm}$ ,  $b=250.46\text{mm}$ ,  $c=83.46\text{mm}$

### Boundary conditions

Bending, shear, and torsion loads were applied at the end of the left fuselage section by means of a RBE2 rigid element linking central node and all other free end nodes shown in Figure 12. The functionality of this element is to smear the loads at the central node across the whole cross-section so as to reduce the local loading effect. The opposite end was fixed but can freely expand in the radial direction due to the difference in pressure inside and outside the fuselage.

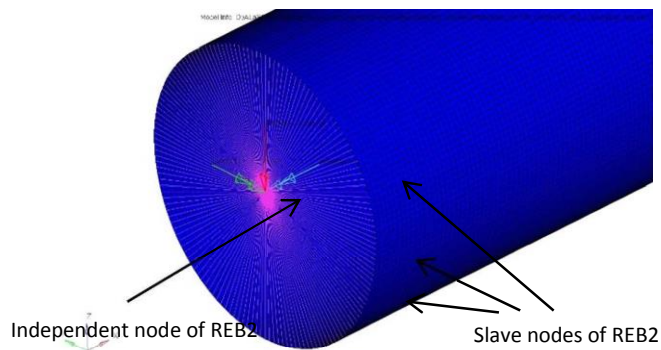


Figure 12 RBE2 rigid element

### Lattice fuselage design of a forward-swept wing aircraft

By applying Eq. (1), the fuselage design by topology optimization was formulated below:

*Objective:* Minimize the compliance of the fuselage,

*Design variables:* Artificial material density  $q$  for each finite element in the designable area,

*Constraints:* Volume fraction:  $\frac{V_0}{V_n} \leq 0.3$

where the left end of the fuselage was applied by the loads including torque, bending and shear; the right end was fully fixed except for the radial displacement; structural masses were applied as distributed loads on the whole barrel. To represent the function of the skin for pressurized and load bending fuselage as well as obtain the efficient pattern of reinforcements, a minimum thickness (0.1mm) is assigned to the skin to simulate its membrane function, however bending loads are mostly carried by stiffeners, whose arrangements are driven by topology optimization for maximal load-carrying capability.  $V_n$  was the volume of finite elements involved in each iteration of the optimization process and  $V_0$  was the maximum volume of the designable structure.

### Lattice design of the fuselage section without windows

Since the Load Case 1 (LC1, downwards loads related) represents the critical driving loads, it should produce the highest corresponding compliance among all the load cases. Hence, loads from LC1 were applied to investigate the efficient pattern of reinforcement on the skin of the fuselage section. Using OptiStruct, the optimal results of the fuselage barrel modelled with structural elements (2D shell and 1D beam) were given in Figure 13. By 2D shell element modelling, the angle of rib-like stiffeners at the mid-surface of the skin parallel to the fuselage axis is measured as approximate 38 degree, which agrees with 40 degree predicted by Central Aerohydrodynamic Institute's (TsAGI). In terms of 1D beam element modelling, a clear pattern of criss-cross stiffeners can also be observed in Figure 13. It is not surprised to identify many horizontal paths of beam elements near the upper and lower extremities of the fuselage cross-section, which will function as the load-carrying backbones. For topology optimization under multi-load cases, the optimal results of the models with 2D shell and 1D beam elements were shown in Figures 14 and 15, respectively.

Since LC1, the critical load case, drives the lattice design of the fuselage, the optimal results from the multi-load case optimization maintain the similarities with the ones from LC1. The differences of the results between them are: 1) More horizontal reinforcements have emerged in a more clear form, and 2) A backbone in Figure 14 is observed at the mid-surface of the skin parallel to the fuselage axis due to the sideways loads (Load case 2) considered in the multi-load case study. This has been also reflected on the result obtained by 1D beam element modelling in Figure 15, which indicates more horizontal paths of beam elements at the rear of the fuselage to bear the larger  $z$ -direction bending moment as compared with the result in Figure 13.

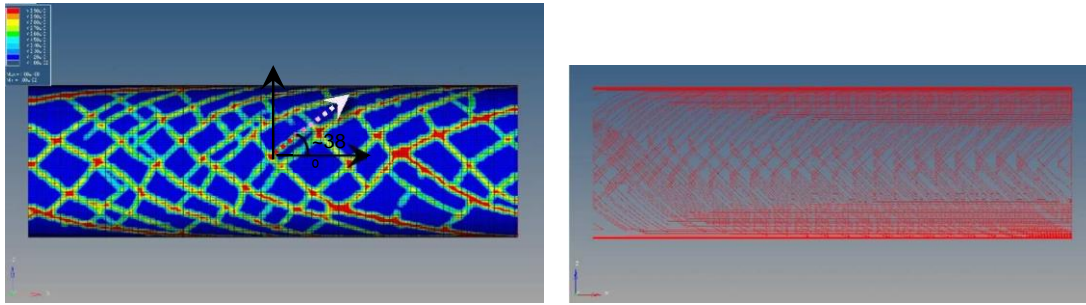


Figure 13 Side view of the optimal reinforcement pattern under LC1:  
2D shell (left) and 1D beam (right)

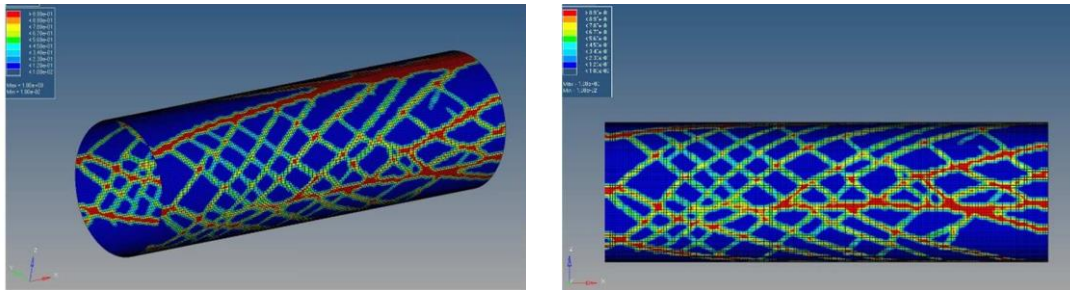


Figure 14 Pattern of optimal reinforcement under multi-load cases with 2D shell element modelling, Iso view (left) and side view (right)

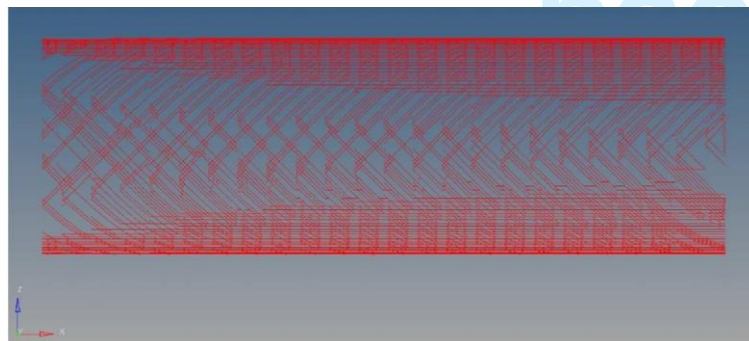


Figure 15 Side view of the optimal reinforcement pattern under multi-load cases with 1D beam element modelling

### Lattice design of the fuselage section with windows

In order to investigate the effect of cut-outs on the efficient reinforcement layout of the fuselage, topology optimization of the fuselage section with cut-outs was performed in this section. For the fuselage barrel with the pitch length of 584.2mm, the shape, the position, and the number of cut-outs (22) were described in Figures 10 and 11. Regarding LC1, it is worth noting that clearer formation and higher density of criss-cross stiffeners surrounding the window areas were identified in Figure 16 than those in Figure 13. This can be explained with the more lattice structures required to transfer loads to the backbones in the regions near the windows. For the fuselage model with 2D shell elements, the angle of truss-like stiffeners passing the window locations indicates about 38 degree shown in Figure 16 and agrees with the angle observed in Figure 13. However, the angle of criss-cross stiffeners around the window locations is 45 degree for the fuselage modeled with 1D beam elements. It is because only 0, 90, and 45 degrees are used when modelling the fuselage with 1D beam elements. This obviously restricts the design space with more constraints as compared to the one for the optimization with 2D shell elements. In the multi-load case study, the higher density of lattice structures around the window locations was formed in Figure 17 than the result shown in Figure 16 and again, the backbone at the mid-surface of the skin parallel to the fuselage axis is observed as well. For the fuselage modelled with 1D beam elements, the optimal patterns of reinforcement (lattice element) on the barrel skin without and with windows under the multi-load case were shown in Figures 15 and 18, respectively. A very distinctive feature which has been presented as a consequence of the topology optimization process can be concluded that the high density for criss-cross stiffeners and horizontal paths of the beam elements can be observed near the rear of the fuselage, then it is gradually reduced along the fuselage axis to the front end due to the smaller bending moments applied. This agrees well with the result from the Michell cantilever study.

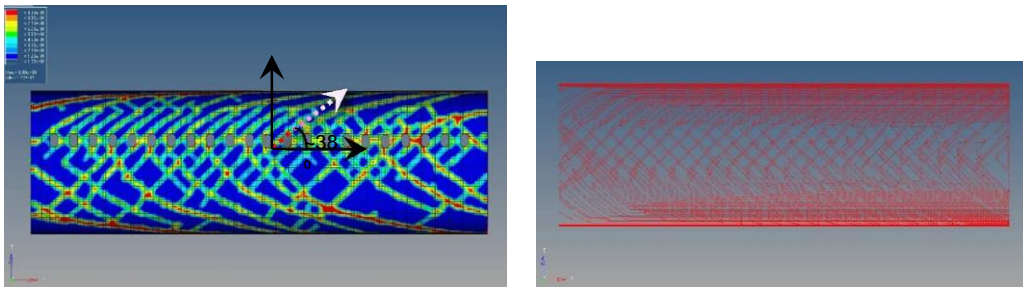


Figure 16 Side view of the optimal reinforcement pattern under LC1:

In use of 2D shell (left) and 1D beam (right) elements to model the fuselage with windows

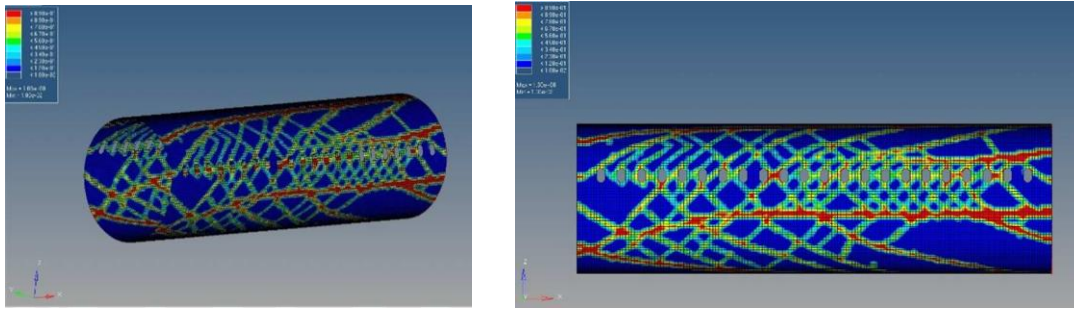


Figure 17 Pattern of optimal reinforcement under multi-load cases in use of 2D shell element to model the fuselage with windows, Iso view (left) and side view (right)



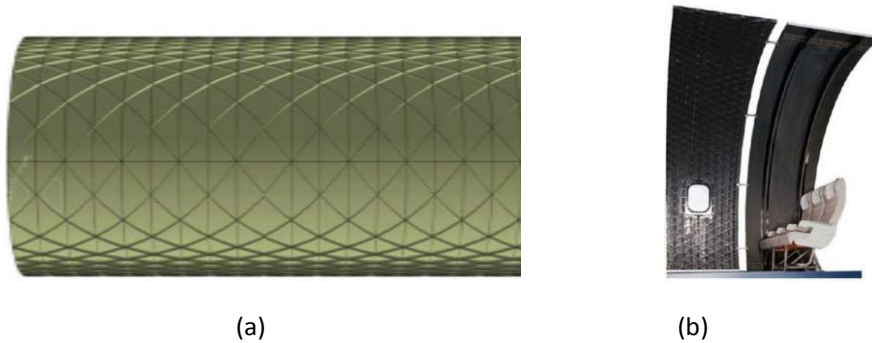
Figure 18 Side view of the optimal reinforcement pattern under multi-load cases in use of 1D beam element to model the fuselage with windows

### *Practical design of the lattice fuselage*

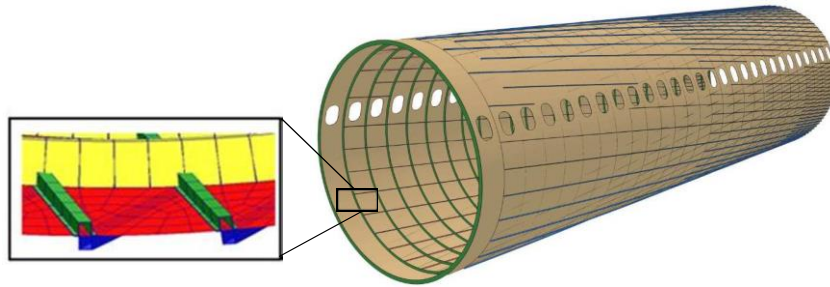
Actually, the lattice stiffeners are very complex and expensive to manufacture due to their continual varying sizes in the design process as well as other constraints, for example, buckling constraint. Based on the optimal layouts of the reinforcements in Figures 14-15 and 17-18 for the fuselage without and with cutouts respectively, the ideally representative pattern of varying angle stiffeners can be depicted in Figure 19(a) and its practical design was reflected by CRISM-DLR demonstrator shown in Figure 19(b). Taking into account manufacturing costs of the lattice structures, it is reasonable to simplify these stiffeners with constant angle accordingly, then align them along geodesic lines on the inside and outside of the fuselage skin shown in Figure 20. Another feature of such lattice fuselage is demonstrated by the varying density distribution of the stiffeners along the fuselage axis due to bending loads increased from the front of the fuselage to the rear. Obviously, the lattice fuselage structure in Figure 20 is much easier and less expensive to



1  
2  
3 be produced and also beneficial from a structural mechanics point of view due to avoidance of  
4 secondary bending of the stiffeners.  
5  
6  
7



20  
21  
22 Figure 19 (a) Fuselage featured by continually varying angle stiffener arrangement;  
23 (b) A full-scale CFRP demonstrator  
24



40 Figure 20 Barrel with constant angled stiffeners and different stiffener density from the front to the  
41 rear  
42

#### 43 **Conclusions**

44  
45  
46 A new lattice fuselage design of a forward-swept wing aircraft was developed in this paper.  
47 Topology optimization was performed to determine the conceptual design of a fuselage barrel  
48 section modelled with 1D beam and 2D shell elements, respectively. The topological results  
49 revealed the need for horizontal stiffeners to be concentrated near the upper and lower  
50 extremities of the fuselage cross section and a lattice pattern of criss-cross stiffeners should be  
51 well-placed along along the sides of the fuselage and near the regions of window locations. The  
52 slight influence of windows on the optimal reinforcement layout was observed, but the clearer  
53 lattice pattern was identified for the fuselage with cut-outs. To obtain clear criss-cross stiffeners,  
54 modelling the fuselage with 1D beam elements is suggested, but the more computational time is  
55 required due to the larger numbers of elements and nodes as compared to those in the model with  
56 2D shell elements. Since a limited number of angles, for example 0, 90, and 45 degrees, are used to

1  
2  
3 model the fuselage with 1D beam elements, the optimal layout of criss-cross stiffeners can only be  
4 presented by the given orientations of the beam elements, while the optimization of the fuselage  
5 modelled by 2D shell elements can form more accurate paths for reinforcements due to a larger  
6 design space. It is concluded that the optimal designs of the fuselage structures by 1D beam and 2D  
7 shell elements have an overall good agreement and this demonstrates the correctness of such a  
8 lattice fuselage concept for the design of forward-swept wing aircrafts. This conceptual design of  
9 lattice stiffeners was first validated by CRISM-DLR demonstrator, and then, inspired by the optimal  
10 designs of stiffeners for the fuselage modelled with 1D beam and 2D shell elements, a lattice barrel  
11 with constant angled stiffeners and different stiffener density from the front to the rear is  
12 developed by DLR. Finally, using topology optimization as a design tool, the obtained optimal lattice  
13 layout of the stiffeners is distinctive to the conventional semi-monocoque fuselage design and also  
14 provides valuable insights into the more efficient utilization of composite materials for novel  
15 aircraft designs.  
16  
17

### 18 19 Declaration of conflicting interests

20  
21  
22 The authors declare that there is no conflict of interest regarding the publication of this paper.  
23  
24  
25

### 26 Acknowledgments

27  
28  
29 The authors acknowledge the support of the European Commission (Dr C. Huehne, DLR) and the  
30 Russian government (Dr A. Shanygin, TsAGI) within the Advanced Lattice Structures for Composite  
31 Airframes (ALaSCA) research project.  
32  
33  
34

### 35 References

- 36  
37 Airframe (2012), *Aviation Maintenance Technician Handbook*, Vol.1, U.S. Department of  
38 Transportation.
- 39  
40 ALaSCA (2013), "Advanced Lattice Structures for Composite Airframes", Project Reference: 265881,  
41 Available: [http://cordis.europa.eu/project/rcn/97744\\_en.html](http://cordis.europa.eu/project/rcn/97744_en.html).
- 42  
43 Altair OptiStruct (2013), V12.0. <http://www.altairhyperworks.com/product/OptiStruct>
- 44  
45 Anand, A., Kapdi, S., M D Jinto, M.D., and Bhuwal, A. (2016), "Light weight structures – application  
46 of topology optimization using stress limit as a criteria in formulation", *International NAFEMS*  
47 *Conference on Engineering Modeling, Analysis, Simulation and 3D Printing*, 29-31 August  
48 2016, Bangalore, India.
- 49  
50 Bendsøe. M.P. (1989). "Optimal shape design as a material distribution parameter problem", *Struct.*  
51 *Optim.*, Vol. 1, pp. 193-202.
- 52  
53 Bendsøe, M. and Sigmund, O. (2003), *Topology Optimization: Theory, Methods and Applications*,  
54 Springer.



- 1  
2  
3 Daniel, I.M. and Ishai, O. (2005), *Engineering Mechanics of Composite Materials*, 2nd ed., Oxford  
4 University Press.  
5  
6 Deaton, J.D. and Grandhi, R.V. (2014), "A survey of structural and multidisciplinary continuum  
7 topology optimization: post 2000", *Structural and Multidisciplinary Optimization*, Vol. 49, pp.1-  
8 38.  
9  
10 Harzheim, L. and Graf, G. (2005), "A review of optimization of cast parts using topology  
11 optimization - Part 1", *Structural and Multidisciplinary Optimization*, Vol. 30 (6), pp. 491-497.  
12  
13 Herbeck, L., Wilmes, H.R., Kolesnikov, B., and Kleineberg, M. (2003), "Technology and design  
14 development for a cfrp fuselage", *25th SAMPE Europe Conference*, Paris, France.  
15  
16 James, K.A., Kennedy, G.J., and Martins, J.R.R.A. (2014), "Concurrent aerostructural topology  
17 optimization of a wing box", *Computers and Structures*, Vol. 134, pp. 1-17.  
18  
19 Kolesnikov, B. and Herbeck, L. (2004), "Carbon fiber composite airplane fuselage: concept and  
20 analysis", *Conference: Merging the Efforts: Russia in European Research Programs on*  
21 *Aeronautics*, Berlin, Germany, pp. 1-11.  
22  
23 Krog L., Tucker A., Kemp, M., and Boyd, R. (2004), "Topology optimization of aircraft wing box ribs",  
24 In: *10th AIAA/ISSMO multidisciplinary analysis and optimization conference*, AIAA Paper: 2004-  
25 4481, AIAA/ISSMO, Albany, USA  
26  
27 Krog, L., Tucker, A., and Rollema, G. (2002), "Application of topology, sizing and shape optimization  
28 methods to optimal design of aircraft components", *Proc. 3rd Altair UK HyperWorks Users*  
29 *Conference*.  
30  
31 Michell A.G.M. (1904), "The limits of economy of material in frame structures", *Phil Mag Ser 6*, Vol.  
32 8(47), pp.589-597.  
33  
34 Mlejnek, H.P. (1992), "Some aspects of the genesis of structures", *Struct. Optim.*, Vol. 5, pp. 64–69.  
35  
36 Niemann, S., Kolesnikov, B., Lohse-Busch, H., Huehne, C., Querin, Q.M., Toropov, V.V., and Liu, D.  
37 (2013), "The use of topology optimisation in the conceptual design of next generation lattice  
38 composite aircraft fuselage structures", *Aeronautical Journal*, Vol.117, pp.1139-1154.  
39  
40 Ostrower, J. (2011), "Boeing to miss 787 performance spec: Albaugh", 15 March 2011.  
41 [https://www.flightglobal.com/news/articles/boeing-to-miss-787-performance-spec-albaugh-](https://www.flightglobal.com/news/articles/boeing-to-miss-787-performance-spec-albaugh-354340/)  
42 [354340/](https://www.flightglobal.com/news/articles/boeing-to-miss-787-performance-spec-albaugh-354340/)  
43  
44 Prager, W. (1974), "A note on discretized Michell structures", *Computer Methods in Applied*  
45 *Mechanics and Engineering*, Vol. 3(3), pp. 349-355.  
46  
47 Quilter, A. (2004), "Composites in aerospace applications", An IHS White Paper,  
48 <http://www.aviationpros.com/article/10386441/composites-in-aerospace-applications>  
49  
50 Rao, J.S., Kiran, S., Chandra, S., Kamesh, J.V., and Padmanabhan, M.A. (2008), "Topology  
51 optimization of aircraft wing", *HyperWorks Technology Conference 2008*, 31 July-02 August  
52 2008, Bangalore, India.  
53  
54 Rozvany, G.I.N. (1998), "Exact analytical solutions for some popular benchmark problems in  
55 topology optimization", *Structural and Multidisciplinary Optimization*, Vol. 15, pp. 42-48.  
56  
57  
58  
59  
60

- 1  
2  
3 Rozvany, G.I.N., Bendsøe, M.P., and Kirsch, U. (1995), "Layout optimization of structures", *Applied*  
4 *Mechanics Reviews*, Vol. 48(2), pp. 41-119.  
5
- 6 Rozvany, G.I.N., Zhou, M., and Gollub, W. (1993), "Layout optimization by COC methods: analytical  
7 solutions", *Proc. NATO ASI Series*, Vol.231, pp. 77-102.  
8
- 9 Russell, H.T., Burley, C.L., and Olson, E. D. (2010), "Hybrid wing body aircraft system noise  
10 assessment with propulsion airframe aeroacoustic experiments", *16th AIAA/CEAS Aeroacoustics*  
11 *Conference*, Stockholm, Sweden, 7-9 Jun, AIAA Paper 2010-3913.  
12
- 13 Seitz, A., Bijewitz, J., Kaiser, S., and Wortmann, G. (2014), "Conceptual investigation of a propulsive  
14 fuselage aircraft layout", *Aircraft Engineering and Aerospace Technology: An International*  
15 *Journal*, Vol. 86 (6), pp. 464-472.  
16
- 17 Seitz, A., Kruse, M., Wunderlich, T., Bold, J., and Heinrich, L. (2011), "LamAiR: Design of a NLF  
18 forward swept wing for short and medium range transport application", *29th AIAA Applied*  
19 *Aerodynamics Conference*, Honolulu, Hawaii, 27-30 June, AIAA2011-3526.  
20
- 21 Shanygin, A., Fomin, V., and Kondakov, I. (2012), "Designing pro-composite aircraft concepts and  
22 layouts to maximise potential benefits of high specific strength of CFRP", *28th Congress of the*  
23 *International Council of the Aeronautical Sciences*, Brisbane, Australia, 23-28 September, Paper:  
24 ICAS 2012-1.7.3.  
25
- 26 Sigmund, O. (2001). "A 99 line topology optimization code written in MATLAB", *Struct. Multidiscip.*  
27 *Optim.*, Vol. 21, pp. 120-127.  
28
- 29 Vasiliev, V.V., Barynin, V.A., and Rasin, A.F. (2001), "Anisogrid lattice structures - survey of  
30 development and application", *Composite Structures*, Vol. 54, pp.361-370.  
31
- 32 Vasiliev, V.V., Barynin, V.A., and Rasin, A.F. (2012), "Anisogrid composite lattice structures -  
33 development and aerospace applications", *Composite Structures*, Vol. 94, pp.1117-1127.  
34
- 35 Vasiliev, V.V. and Rasin, A.F. (2006), "Anisogrid composite lattice structures for spacecraft and  
36 aircraft applications", *Composite Structures*, Vol. 76, pp.182-189.  
37
- 38 Wilmes, H., Kolesnikov, B., Fink, A., and Kindervater, C. (2002), "New design concepts for a cfrp  
39 fuselage", *Workshop on Final Project of Black Fuselage*, Braunschweig, Germany.  
40
- 41 Zhou, M., Fleury, R., and Kemp, M. (2010), "Optimization of Composite – Recent Advances and  
42 Application", *13th AIAA/ISSMO Multidisciplinary Analysis Optimization Conference,*  
43 *Multidisciplinary Analysis Optimization Conferences*, AIAA Paper: 2010-9272, Texas, USA  
44
- 45 Zhou, M., Fleury, R., Shyy, Y.K., Thomas, H., and Brennan, J.M. (2002), "Progress in topology  
46 optimization with manufacturing constraints", *Proc. of the 9th AIAA/ISSMO symposium on*  
47 *multidisciplinary analysis and optimization*, Atlanta, pp. 1-8.  
48
- 49 Zhou, M., Rozvany, G.I.N. (1991), "The COC algorithm, Part II: topological, geometry and  
50 generalized shape optimization", *Comp. Meth. Appl. Mech. Engrg.*, Vol. 89, pp. 197-224.  
51
- 52 Zhu, J.H., Zhang, W.H., Xia, L. (2016), "Topology optimization in aircraft and aerospace structures  
53 design", *Archives of Computational Methods in Engineering*, Vol. 23 (4), pp. 595-622.  
54  
55  
56  
57  
58  
59  
60